

## Validation of vertical ground reaction forces on individual limbs calculated from kinematics of horse locomotion

Maarten F. Bobbert<sup>1,\*</sup>, Constanza B. Gómez Álvarez<sup>2</sup>, P. René van Weeren<sup>2</sup>, Lars Roepstorff<sup>3</sup> and Michael A. Weishaupt<sup>4</sup>

<sup>1</sup>*Institute for Fundamental and Clinical Human Movement Sciences, Vrije Universiteit, van der Boechorstraat 9, NL-1081 BT Amsterdam, The Netherlands,* <sup>2</sup>*Department of Equine Sciences, Faculty of Veterinary Medicine, Utrecht University, Yalelaan 12, NL-3584 CM Utrecht, The Netherlands,* <sup>3</sup>*Department of Equine Studies, Swedish University of Agricultural Sciences, 750 05 Uppsala, Sweden and* <sup>4</sup>*Equine Hospital, Vetsuisse Faculty, University of Zurich, Winterthurerstrasse 260, CH-8057 Zurich, Switzerland*

\*Author for correspondence (e-mail: [M\\_F\\_Bobbert@fbw.vu.nl](mailto:M_F_Bobbert@fbw.vu.nl))

Accepted 7 March 2007

### Summary

The purpose of this study was to determine whether individual limb forces could be calculated accurately from kinematics of trotting and walking horses. We collected kinematic data and measured vertical ground reaction forces on the individual limbs of seven Warmblood dressage horses, trotting at  $3.4 \text{ m s}^{-1}$  and walking at  $1.6 \text{ m s}^{-1}$  on a treadmill. First, using a segmental model, we calculated from kinematics the total ground reaction force vector and its moment arm relative to each of the hoofs. Second, for phases in which the body was supported by only two limbs, we calculated the individual reaction forces on these limbs. Third, we assumed that the distal limbs operated as linear springs, and determined their force–length relationships using calculated individual limb forces at trot. Finally, we calculated individual limb force–time histories from distal limb lengths. A good correspondence was obtained between calculated and

measured individual limb forces. At trot, the average peak vertical reaction force on the forelimb was calculated to be  $11.5 \pm 0.9 \text{ N kg}^{-1}$  and measured to be  $11.7 \pm 0.9 \text{ N kg}^{-1}$ , and for the hindlimb these values were  $9.8 \pm 0.7 \text{ N kg}^{-1}$  and  $10.0 \pm 0.6 \text{ N kg}^{-1}$ , respectively. At walk, the average peak vertical reaction force on the forelimb was calculated to be  $6.9 \pm 0.5 \text{ N kg}^{-1}$  and measured to be  $7.1 \pm 0.3 \text{ N kg}^{-1}$ , and for the hindlimb these values were  $4.8 \pm 0.5 \text{ N kg}^{-1}$  and  $4.7 \pm 0.3 \text{ N kg}^{-1}$ , respectively. It was concluded that the proposed method of calculating individual limb reaction forces is sufficiently accurate to detect changes in loading reported in the literature for mild to moderate lameness at trot.

Key words: *Equus caballus*, trot, walk, biomechanics, limb stiffness, model, duty factor.

### Introduction

Performance horses commonly suffer from musculoskeletal injuries. These injuries will typically result in lameness, which will interfere with training and competition, and they constitute an important cause of wastage of performance horses (Jeffcott et al., 1982; Rosedale et al., 1985). The impact on the equine industry is huge. For example, in 1998 economic losses due to musculoskeletal injury in the Thoroughbred racehorse were estimated at US\$ one billion in the United States alone (Kobluk, 1998). Obviously, early diagnosis and treatment of lameness is important, both from an animal welfare perspective and from an economic perspective.

In the diagnosis of musculoskeletal injuries, the eye of the clinician is an invaluable tool. However, objective measures may have added value. Kinematic analysis has been used to provide quantitative data on locomotion patterns of healthy and

lame horses (e.g. Buchner et al., 1996a; Buchner et al., 1996b; Buchner et al., 2001; Clayton et al., 2000; Galisteo et al., 1997; Keegan et al., 1998; Keegan et al., 2000; Kramer et al., 2000; Uhlir et al., 1997). Information about the forces on the individual limbs is highly desirable for diagnosis and evaluation of treatments, and also seems indispensable to further our understanding of adaptations of the locomotion patterns following injury. After all, the adaptations will be intended to reduce the load on the injured structures. As holds for studying locomotion in general, it is highly desirable to have both forces on the individual limbs and whole-body kinematics, so that changes in the forces can be linked to changes in the locomotion pattern.

Various methods of obtaining information on individual limb forces have been developed, each of which has advantages and disadvantages. First of all, force plates can be used (e.g.

Clayton et al., 2000; Merckens and Schamhardt, 1988; Merckens et al., 1986; Morris and Seeherman, 1987; Schamhardt and Merckens, 1987; Schamhardt et al., 1986). A force plate provides full information on the ground reaction force vector, but a disadvantage is that it can measure the force of only one limb at a time. Moreover, capturing a clean hit of the force platform with the limb of interest may require two to six attempts, depending on the variability of the horse and the type of gait studied (Merckens et al., 1986; Merckens et al., 1993a; Merckens et al., 1993b). A second method to obtain individual limb forces is to use instrumented horseshoes (Barrey, 1990; Kai et al., 2000; Roepstorff and Drevemo, 1993). This solves the problem of getting the horse to hit a force plate with the limb of interest and allows for the study of many consecutive strides. The early instrumented horseshoes were fragile and did not provide full information on the ground reaction force, but a recently developed dynamometric horseshoe (Roland et al., 2005) seems robust and accurately provides the six components of the load. However, if measurements are to be made on a horse, this horse will need to be shod with instrumented shoes, and because the mass of the instrumented horseshoes is greater than that of normal horseshoes, the stride variables to be studied could be affected (Roland et al., 2005). A third method of obtaining information on the ground reaction force has been presented by Weishaupt and colleagues (Weishaupt et al., 2002; Weishaupt et al., 2004a; Weishaupt et al., 2004b; Weishaupt et al., 2006). They devised a treadmill the support surface of which was mounted on 18 force sensors, allowing for simultaneous measurement of the vertical ground reaction forces on each of the four limbs over multiple strides. This method requires minimal instrumentation of the horse, but a slight downside is that the horse needs to be accustomed to treadmill locomotion, and unfortunately the system does not provide the full reaction force vectors. Also, slight differences have been reported in kinematic patterns during treadmill locomotion and kinematics during overground locomotion (Buchner et al., 1994), but it cannot be excluded that these were due to differences in the properties of the support surface.

Instead of directly measuring ground reaction forces on the individual limbs of the horse, it can be attempted to estimate them from kinematics. A method to do so has been proposed by McGuigan and Wilson (McGuigan and Wilson, 2003). The method builds on the observation that the distal forelimb of the horse behaves like a spring, i.e. the force carried by the limb is directly related to the distance between the elbow and the hoof, and also to the fetlock joint angle (McGuigan and Wilson, 2003). This means that the latter two kinematic variables can be used as a type of 'strain gauge', provided that they have been calibrated, i.e. that the relationship between limb force and elbow-hoof distance or fetlock angle is known. For this calibration, McGuigan and Wilson (McGuigan and Wilson, 2003) used kinematic data collected simultaneously with force plate data at trot. Then, using fetlock angles measured during gallop, they applied the calibration results to estimate the peak vertical ground reaction forces on the individual forelimbs.

The method developed by McGuigan and Wilson

(McGuigan and Wilson, 2003) is elegant and involves no interference with the horse other than the application of markers defining the kinematic variables to be used in force calculations. Also, it can be applied to overground locomotion. However, the calibration requires the use of a force platform, and therefore suffers from the associated disadvantages. An indirect approach to calibration would be to use limb forces estimated from duty factor, with the duty factor of a limb being the proportion of the stride for which that limb is in contact with the ground (Alexander et al., 1979; Witte et al., 2004). It has been shown that at trot, peak vertical ground reaction forces for individual limbs could be predicted from duty factor with errors of only 3% (Witte et al., 2004). The predicted peak forces at trot could be used for calibration of the 'strain gauges', and the calibrated 'strain gauges' could be used to determine forces at other gaits. However, the calculation of forces from duty factors, henceforth referred to as 'duty factor method', relies on information about the distribution of the total ground reaction force over the individual limbs, which must have been acquired in previous research with the help of direct force measurements. Furthermore, it involves assumptions about symmetry and periodicity that will not hold in lame horses.

It would be ideal if calibration of the 'strain gauges' could be achieved using kinematic data collected for analysis of the locomotion pattern. In principle, such data allow for calculation of individual limb forces for phases during locomotion in which only two limbs are simultaneously in contact with the ground. After all, kinematic data can be used to calculate the acceleration of the centre of mass of the horse, and hence the magnitude and direction of the total ground reaction force vector. As explained in Fig. 1, this information can be combined with the rate of change of angular momentum of the horse, also calculated from the kinematic data, to determine the moment arms of the total ground reaction force relative to the two supporting hoofs (Bobbert and Santamaria, 2005). The ratio of these moment arms then gives an indication of the relative contribution of each of the supporting limbs to the total ground reaction force, so the individual limb forces can be calculated. The forces obtained using this ground reaction force distribution method, henceforth referred to as 'GRF distribution method', can then be combined with distal limb length or fetlock angle for the calibration of these indicators of limb force. Finally, given the results of the calibration, time histories of individual limb forces can be estimated from time histories of distal limb length or fetlock angle. From a mechanical point of view this approach is straightforward, but it seems a long shot and the question may be raised whether it produces accurate results when real-world kinematic data are used. One of the problems, for example, is that markers placed on the skin may move considerably relative to the underlying bony landmarks (van Weeren and Barneveld, 1986; van Weeren et al., 1988; van Weeren et al., 1990a; van Weeren et al., 1990b), causing errors in the force calculations.

The purpose of this study was to determine whether individual limb forces can be calculated accurately from kinematics of trotting and walking horses. For this purpose we

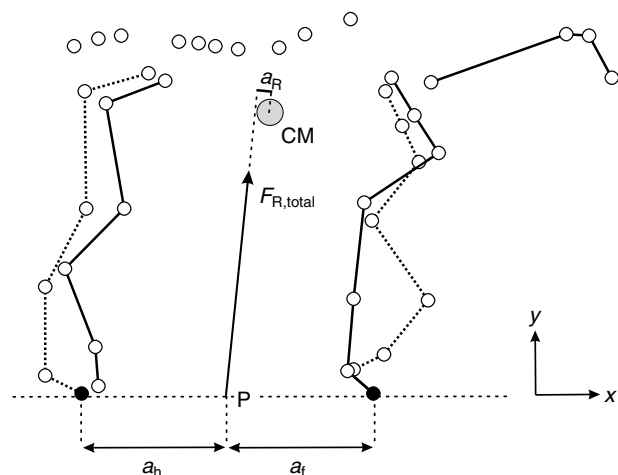


Fig. 1. Location of markers and explanation of the GRF distribution method. Retroreflective markers (small circles) were placed bilaterally on the skin overlying bony landmarks of the forelimb (tuber of spina scapulae, greater tubercle of humerus, a point midway between the two, lateral epicondyle of humerus, carpal joint, fetlock joint, lateral side of the hoof at the level of the coffin joint), hindlimb (tuber coxae, greater trochanter of femur, lateral epicondyle of femur, tarsal joint, fetlock joint, lateral side of the hoof at the level of the coffin joint), and on the head and neck (crista facialis, zygomatic arc, wing of atlas, transverse process of vertebra C7). Furthermore, spherical markers were placed on the trunk (spinous processes of vertebrae T6, T10, T13, T17, L1, L3, L5, S3, S5 and C2). Left limbs are indicated with dotted lines, markers on hoofs in contact with the ground have been filled. The GRF distribution method involved the following steps. The acceleration of the centre of mass (CM) of the horse was calculated from the marker position–time histories using a segmental model. The acceleration of CM, combined with the acceleration due to gravity, provided the magnitude and direction of the calculated total ground reaction force vector  $F_{R,total}$ . The product of the ground reaction force and its moment arm relative to CM ( $a_R$ ) equals the rate of change of angular momentum. The latter was also calculated from marker position–time histories, so  $a_R$  could be calculated. This then fully defined the line of action of the calculated  $F_{R,total}$ , and therewith the point P where it passed between the hoofs of the limbs in contact with the ground. When only one forelimb and one hindlimb were in contact with the ground, the relative contribution of the forelimb to the calculated  $F_{R,total}$  was taken to be equal to  $a_f/(a_f+a_h)$  and that of the hindlimb was taken to be equal to  $a_h/(a_f+a_h)$ . The situation shown in the diagram occurred at the instant that the vertical component of  $F_{R,total}$  ( $F_{Ry,total}$ ) reached its peak at trot (for illustrative purposes a trial was selected in which the angular momentum and horizontal component of  $F_{R,total}$  were exceptionally large at the instant that  $F_{Ry,total}$  attained its peak).

calculated, as outlined in the previous paragraph, individual limb forces from kinematics collected while horses were walking and trotting on an instrumented treadmill (Weishaupt et al., 2002). To evaluate the accuracy of the calculated forces, we compared them with vertical reaction forces of the individual limbs provided by the treadmill-integrated force measuring system. We also compared the individual limb

forces calculated from kinematics with forces calculated from duty factors of the limbs.

### Materials and methods

The experiments were carried out at the Equine Hospital, University of Zurich, Switzerland. The experimental protocol had been approved by the Animal Health and Welfare Commission of the canton of Zurich. Seven sound Warmblood dressage horses *Equus caballus* L., six geldings and one stallion, participated in the study. Age of the horses was  $14 \pm 4$  yr, mass was  $609 \pm 62$  kg and height, measured at the withers, was  $1.70 \pm 0.07$  m. The horses had to walk and trot on a high-speed treadmill (Mustang 2200, Kagra AG, Fahrwangen, Switzerland) with an integrated force measuring system (Weishaupt et al., 2002), to which they had been accustomed prior to the day of the measurements. For the current study we selected from each horse one walking trial at a speed of  $1.6 \text{ m s}^{-1}$  and one trotting trial at a speed of  $3.4 \text{ m s}^{-1}$ .

The treadmill-integrated force measuring system provided the vertical ground reaction force on each of the limbs ( $F_{Ry,i}$ ) at 480 Hz. For the kinematic analysis, markers were applied to the skin overlying bony landmarks on both sides of the body (Fig. 1). The markers were monitored during stance and locomotion by 12 infrared cameras operating at 240 Hz (Pro Reflex, Qualisys Medical AB, Göteborg, Sweden). Force data and kinematic data were captured simultaneously for a period of 15 s, both at trot and at walk. First, we needed to know the contact phases of each of the limbs. These were determined from the horizontal velocities of the hoofs, obtained by numerical differentiation of the trajectories of the hoof markers after smoothing these at 8 Hz using a fourth-order zero-lag Butterworth filter. Next, we intended to calculate the lengths of the distal limbs from the marker position–time histories and the position and acceleration of the centre of mass. Before performing these calculations, however, we took two precautions that were expected to benefit the validity of the outcome (see also Bobbert and Santamaria, 2005).

First, for the limbs, we attempted to remedy the problem of motion of skin markers relative to the underlying bony landmarks. For this purpose, we assumed that the limbs were chains of interconnected rigid segments (van den Bogert et al., 1994). To define the lengths of the rigid link segments for each of the limbs we used the configuration just before landing in trot. Assuming, furthermore, that no error occurred in measuring the locations of the markers on the hoofs, we optimised, for each individual video frame, the configuration of the chain of each of the limbs by minimizing the sum of squared distances between the locations of the chain joints and the actual marker locations. This also allowed us to solve the problem that occasionally a fetlock marker or a shoulder marker was lost from view during a section of a stride.

The second precaution taken was to define a rigid template for the trunk, using the locations of markers on the trunk in square standing. We also determined the location of the centre of mass of the trunk and of the marker on vertebra C7 relative

to the rigid trunk template in square standing. Subsequently, for each individual video frame, the position and orientation of the template were found by optimisation, using as criterion the sum of weighted squared differences between template marker locations and actual marker locations. The weighting was introduced because the fore–aft excursions of some markers seemed larger than those of the underlying bones (for instance, at trot, the distance between the markers at the level of vertebrae T6 and T10 varied sinusoidally at the step frequency with a peak-to-peak amplitude of up to 2 cm in some horses, which was surely more than the variation in the distance between the spinous processes of vertebrae T6 and T10). The motions of the markers on vertebrae T17, L1, L3 and L5 seemed quite representative of those of the underlying bony landmarks, and therefore the squared differences between the locations of these markers in the template and their actual locations were counted twice in the optimisation criterion. The movement of the centre of mass of the trunk, the trunk orientation, and the location of vertebra C7, were then derived from the movement of the template during locomotion.

The time histories of the marker coordinates, some of which had been reconstructed by fitting of templates, were smoothed at 6 Hz using a fourth-order zero-lag Butterworth filter. Angles of the segments with the horizontal were calculated, and a segmental model (Buchner et al., 1997) was used to determine the locations of mass centres of the limb segments and the head and neck. The combination of these segmental mass centres, weighted according to their relative masses, provided the location of the centre of mass of the whole body (CM). Cubic splines were fitted to position-time and angle-time histories, and the coefficients of the piecewise polynomials were used to obtain linear and angular velocities and accelerations of the individual body segments. This information was then used to calculate the linear acceleration of CM, as well as the rate of change of angular momentum. Furthermore, the coordinates of the joints of the limb chains were used to calculate the distances to be used as indicators of limb force: the distance from elbow to coffin joint in the forelimb, and the distance from stifle joint to coffin joint in the hindlimb.

Individual limb forces were calculated from kinematics as outlined in the introduction for phases in which only two limbs were in contact with the ground. The first step, explained in Fig. 1, was to determine the distribution of the calculated total ground reaction force ( $F_{R,\text{total}}$ ) over the limbs, by determining the point P where the line of action of the calculated total ground reaction force passed between the hoofs. Once P had been found, the calculated  $F_{R,\text{total}}$  was distributed over the individual ground reaction forces  $F_{R,i}$  of the supporting forelimb and the diagonal hindlimb using the inverse ratio of their moment arms. In doing so, it was implicitly assumed that the relative contribution of the two supporting limbs to the horizontal component of the calculated  $F_{R,\text{total}}$  ( $F_{R_x,\text{total}}$ ) is the same as their relative contribution to the vertical component ( $F_{R_y,\text{total}}$ ), or in other words, that the two individual limb reaction forces run in parallel. We are aware that the contributions of the forelimbs and hindlimbs  $F_{R_x,\text{total}}$  may actually be different (Dutto et al.,

2004). However, at trot we were interested primarily in the distribution in the middle of the stance phase, where  $F_{R_x,\text{total}}$  is less than 10% of  $F_{R_y,\text{total}}$  (Dutto et al., 2004; Merkens et al., 1993b; Wilson et al., 2001), so that a violation of our assumption will have only a small effect on the distribution. At walk, the horizontal force is also small compared to the vertical force throughout the cycle (Merkens et al., 1986); we calculated the distribution of  $F_{R_y,\text{total}}$  for several instants that will be specified in the Results section, after presentation of the force–time histories of the individual limbs.

The reaction force on each individual limb calculated at the instant that  $F_{R_y,\text{total}}$  attained its peak at trot, together with the length of the distal limb at this instant, gave us one point on the force–length relationship of the distal limb. For the second point, we used zero force and the distal limb length just before touch-down. With these two points, the linear force–length relationship of each of the distal limbs was defined. This relationship was then used to calculate for each frame  $F_{R,i}$  from the length of the distal limb. In the forelimb,  $F_{R,i}$  was assumed to act along the line from the foot to the attachment of serratus ventralis on the scapula (Dutto et al., 2006; McGuigan and Wilson, 2003), and for comparison with the measured  $F_{R_y,i}$  we multiplied the calculated  $F_{R,i}$  by the sine of the angle of this line with the horizontal. In the hindlimb,  $F_{R,i}$  was assumed to act along the line from the foot to the point mid-way between tuber coxae and trochanter major (Dutto et al., 2006), and for comparison with the measured  $F_{R_y,i}$  we multiplied the calculated  $F_{R,i}$  by the sine of the angle of this line with the horizontal.

To determine the accuracy of calculating peak values of  $F_{R_y,\text{total}}(t)$  at trot, we used the following procedure. First, from the data captured over 15 s we took, for each horse, the first 15 complete stride cycles, starting with touch-down of the left forelimb. For each of the corresponding 15 left-diagonal and 15 right-diagonal stance phases, we determined the peak of the calculated  $F_{R_y,\text{total}}(t)$  as well as the peak of the measured  $F_{R_y,\text{total}}(t)$ , i.e. the sum of the vertical reaction forces of the individual limbs provided by the treadmill-integrated force measuring system. Next, we averaged these peak values over the stance phases to obtain what we will call a ‘mean peak value’ for calculated  $F_{R_y,\text{total}}$  and a ‘mean peak value’ for measured  $F_{R_y,\text{total}}$ , and we took the difference between the elements of each pair. Finally, we took the standard deviation of the differences obtained this way. This standard deviation will be referred to as the between-diagonal standard error of estimate (SEE); it is the standard error that one makes in estimating the peak measured  $F_{R_y,\text{total}}$  for a given diagonal of a given horse in trot on the basis of kinematics. If one is interested only in the variations in peak  $F_{R_y,\text{total}}$  over time, for example in a study in which lameness is temporarily induced (e.g. Buchner et al., 1996a; Weishaupt et al., 2004a), the between-diagonal SEE is not important; in that case the within-diagonal SEE is the parameter of interest. Within-diagonal SEE values were calculated as follows. We subtracted from the peak values of the calculated  $F_{R_y,\text{total}}$  of the individual stance phases the mean peak value, performed the analogous operation for



the peak values of the measured  $F_{Ry,total}$ , and then took the difference between the two elements of each pair. The standard deviation of the differences so obtained will be referred to as the within-diagonal SEE.

Using a procedure analogous to the one described above, we determined the between-limb and within-limb SEE for calculating peak values of  $F_{Ry,i}(t)$  according to the GRF distribution method, and for calculating peak values of  $F_{Ry,i}(t)$  from distal limb length. Furthermore, SEE values were not only calculated for trotting but also for walking, in which case we selected for each horse nine complete stride cycles from the 15 s of data, starting with touch-down of the left forelimb. Last but not least, for several variables we calculated 'grand mean peak values' by averaging not only over stance phases but also over horses.

The question may be raised how the accuracy of calculating peak  $F_{Ry,i}$  according to the GRF distribution method compares with that of calculating peak  $F_{Ry,i}$  according to the duty factor method proposed by others (e.g. Alexander et al., 1979; Witte et al., 2004). To be able to answer this question, we also calculated peak  $F_{Ry,i}$  using the following equation:

$$\text{Peak } F_{Ry,i} = \pi M g p / (2\beta), \quad (1)$$

where  $M$  is the mass of the horse (kg),  $g$  is the acceleration due to gravity ( $9.81 \text{ m s}^{-2}$ ),  $p$  is the proportion of the mass of the animal carried on average by the limb in question, and  $\beta$  is the duty factor, i.e. that fraction of the stride time for which this limb transmits force to the ground. For  $p$  we used fixed values extracted from Witte et al. (Witte et al., 2004): 0.285 for each of the forelimbs and 0.215 for each of the hindlimbs at trot, and 0.295 for each of the forelimbs and 0.205 for each of the hindlimbs at walk. Values for  $\beta$  were extracted from the measured  $F_{Ry,i}(t)$  using a threshold of 100 N.

## Results

Time histories of calculated and measured  $F_{Ry,total}$  are presented for three of the horses in the top panels of Fig. 2 for trotting, and in the top panels of Fig. 3 for walking. The results obtained with these horses were not better than those obtained with the other horses; as a matter of fact, the results obtained with horse 2 were the worst of all. A good correspondence was obtained between calculated and measured  $F_{Ry,total}(t)$  (Figs 2 and 3), and between the mean peak values of the calculated and measured  $F_{Ry,total}(t)$  (Fig. 4). At trot, the grand mean peak  $F_{Ry,total}$  was calculated to be  $21.4 \pm 0.6 \text{ N kg}^{-1}$  and measured to be  $21.7 \pm 0.9 \text{ N kg}^{-1}$ , with the between-diagonal SEE being  $0.5 \text{ N kg}^{-1}$  (note that the between-diagonal SEE is the average absolute distance in the vertical direction between the data points and the line of identity in Fig. 4). Time histories of the calculated horizontal component of  $F_{R,total}$ ,  $F_{Rx,total}$ , could not be evaluated directly because the instrumented treadmill did not provide these. However, they were comparable to results of direct force measurements presented in the literature (Dutto et al., 2004; Merkens et al., 1993b). For example, at trot, the

grand mean minimum value of  $F_{Rx,total}$  (i.e. the peak braking force) amounted to  $-3.2 \pm 0.4 \text{ N kg}^{-1}$  and occurred at  $26 \pm 2\%$  of the stance phase, and the grand mean maximum value of  $F_{Rx,total}$  (i.e. the peak propulsive force) amounted to  $2.9 \pm 0.5 \text{ N kg}^{-1}$  and occurred at  $60 \pm 2\%$  of the stance phase.

At walk, the grand mean peak  $F_{Ry,total}$  was calculated to be  $12.2 \pm 0.4 \text{ N kg}^{-1}$  and measured to be  $12.2 \pm 0.5 \text{ N kg}^{-1}$ , with the between-diagonal SEE being  $0.3 \text{ N kg}^{-1}$  (the peak  $F_{Ry,total}$  at walk does in fact occur during the phase in which the body is supported by one forelimb and the diagonal hindlimb, see Fig. 3). Also, within each horse, the variations in peak  $F_{Ry,total}$  from stride to stride could be traced reasonably well, as exemplified for the trotting trial of one horse in Fig. 5; the within-diagonal SEE, determined using the results for all the limbs of all the horses, was less than  $0.2 \text{ N kg}^{-1}$ , both at trot and at walk. Below, further results are first presented for trotting, and then for walking.

For the calculation of individual limb forces at trot to be successful, the total force needed to be distributed correctly over the forelimb and diagonal hindlimb in contact with the ground. When evaluated at the instant that  $F_{Ry,total}$  reached its peak, the grand mean of the relative load on the forelimb was  $54.1 \pm 3.6\%$  for  $F_{Ry,total}$  calculated from kinematics, and  $54.3 \pm 2.1\%$  for  $F_{Ry,total}$  provided by the treadmill-integrated force measuring system. The distribution of peak  $F_{Ry,total}$  varied somewhat over the horses (see Fig. 2), and there was an acceptable match between the forelimb's calculated relative contribution to peak  $F_{Ry,total}$  and its measured relative contribution to peak  $F_{Ry,total}$  (Fig. 6); the between-diagonal SEE of the distribution was 2.3%. The next step was to combine the distribution over the limbs calculated from kinematics with the calculated  $F_{Ry,total}$ . Fig. 7 shows the resulting mean peak  $F_{Ry,i}$  values together with the mean peak measured  $F_{Ry,i}$  values. At trot, the grand mean peak  $F_{Ry,i}$  in the forelimb was calculated to be  $11.5 \pm 0.9 \text{ N kg}^{-1}$  and measured to be  $11.7 \pm 0.9 \text{ N kg}^{-1}$ , with the inter-limb SEE in the calculated values being  $0.4 \text{ N kg}^{-1}$  and the intra-limb SEE amounting to  $0.3 \text{ N kg}^{-1}$ . In the hindlimb, at trot, the grand mean peak  $F_{Ry,i}$  was calculated to be  $9.8 \pm 0.7 \text{ N kg}^{-1}$  and measured to be  $10.0 \pm 0.6 \text{ N kg}^{-1}$ , with the inter-limb SEE in the calculated values being  $0.7 \text{ N kg}^{-1}$  and the intra-limb SEE amounting to  $0.3 \text{ N kg}^{-1}$ .

Peak  $F_{Ry,i}$  values were not only calculated using the GRF distribution method, but also using the duty factor method (Eqn 1), using fixed values for  $p$  extracted from Witte et al. (Witte et al., 2004) and duty factors  $\beta$  extracted from measured  $F_{Ry,i}(t)$ . Fig. 8 shows the resulting mean peak  $F_{Ry,i}$  values together with the mean peak measured  $F_{Ry,i}$  values. At trot, the grand mean peak  $F_{Ry,i}$  calculated using Eqn 1 was  $11.2 \pm 0.5 \text{ N kg}^{-1}$  in the forelimb, with the inter-limb SEE being  $0.7 \text{ N kg}^{-1}$  and the intra-limb SEE amounting to  $0.16 \text{ N kg}^{-1}$ , and  $9.6 \pm 0.4 \text{ N kg}^{-1}$  in the hindlimb, with the inter-limb SEE being  $0.4 \text{ N kg}^{-1}$  and the intra-limb SEE amounting to  $0.2 \text{ N kg}^{-1}$ . Suffice it to say here that even with error-free  $\beta$ -values [they were error-free because they had been extracted from measured  $F_{Ry,i}(t)$ ], the duty factor method when used to

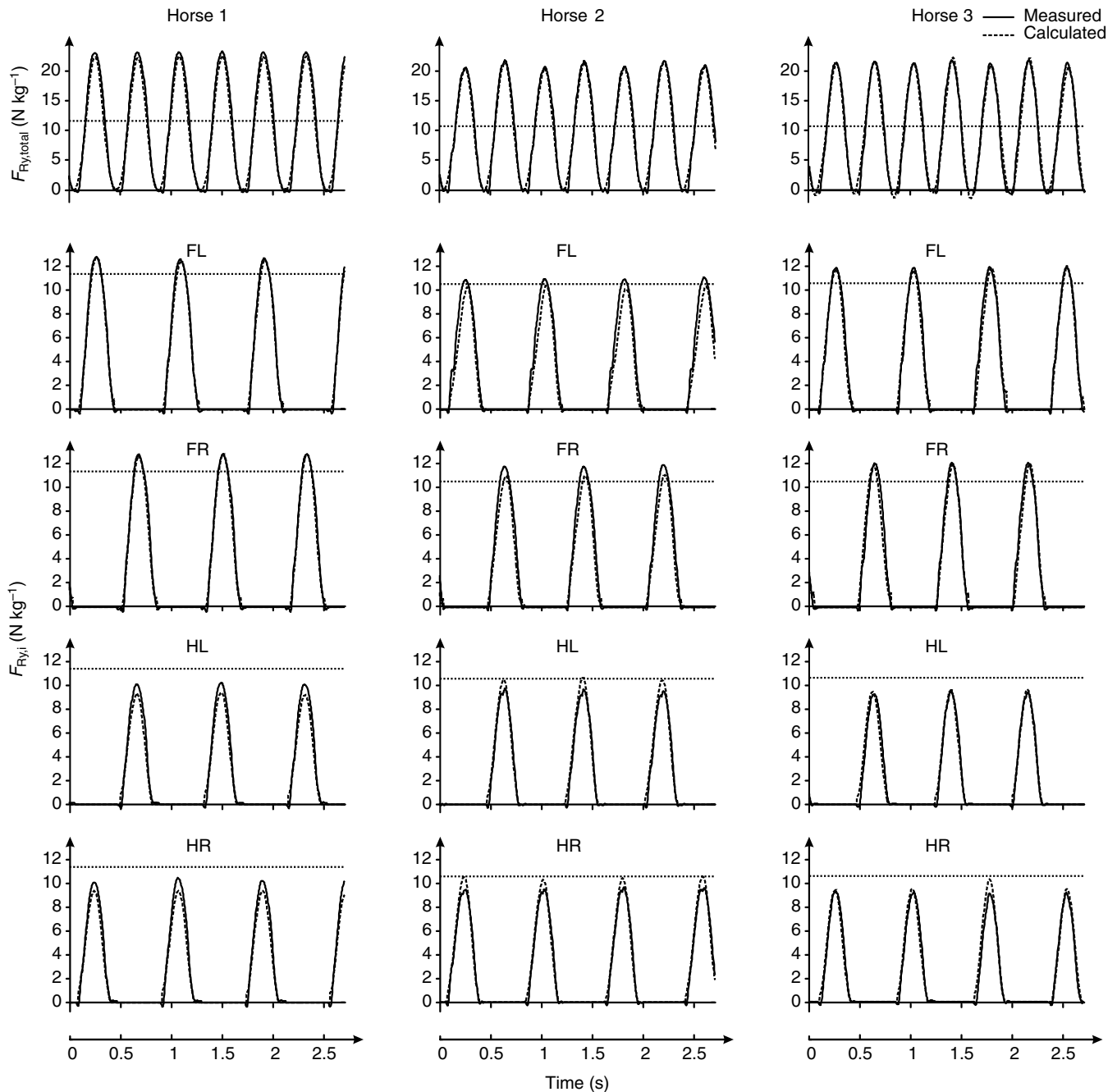


Fig. 2. Time histories of the measured and calculated total vertical ground reaction force ( $F_{Ry,total}$ ), as well as of the measured and calculated vertical ground reaction force on each of the limbs ( $F_{Ry,i}$ ), of three horses at trot. Calculated  $F_{Ry,i}(t)$  were obtained from distal limb lengths, using the force-length relationships of the distal limbs determined with the help of calculated values of  $F_{Ry,i}$  and limb lengths at trot. Dotted horizontal lines indicate half the peak value of  $F_{Ry,total}$ . FL, left forelimb; FR, right forelimb; HL, left hindlimb; HR, right hindlimb.

calculate peak values of  $F_{Ry,i}$  did not clearly outperform the GRF distribution method.

As explained in the Materials and methods section, the peak calculated  $F_{R,i}$  values, obtained according to the GRF distribution method, were used to determine the force-length relationships of the distal limbs, under the assumption that these relationships were linear. The stiffness of the distal forelimb obtained this way was  $130 \pm 16 \text{ N kg}^{-1} \text{ m}^{-1}$  (range:

$101\text{--}156 \text{ N kg}^{-1} \text{ m}^{-1}$ ) and that of the distal hindlimb was  $73 \pm 4 \text{ N kg}^{-1} \text{ m}^{-1}$  (range:  $64\text{--}78 \text{ N kg}^{-1} \text{ m}^{-1}$ ). These force-length relationships were subsequently used to calculate  $F_{R,i}(t)$  from distal limb length-time histories, and combined with limb angle-time histories to obtain  $F_{Ry,i}(t)$  as a function of time. For trotting, the calculated  $F_{Ry,i}(t)$  of three horses are shown together with the measured  $F_{Ry,i}(t)$  in Fig. 2. The match between the calculated and measured curves was quite good (it

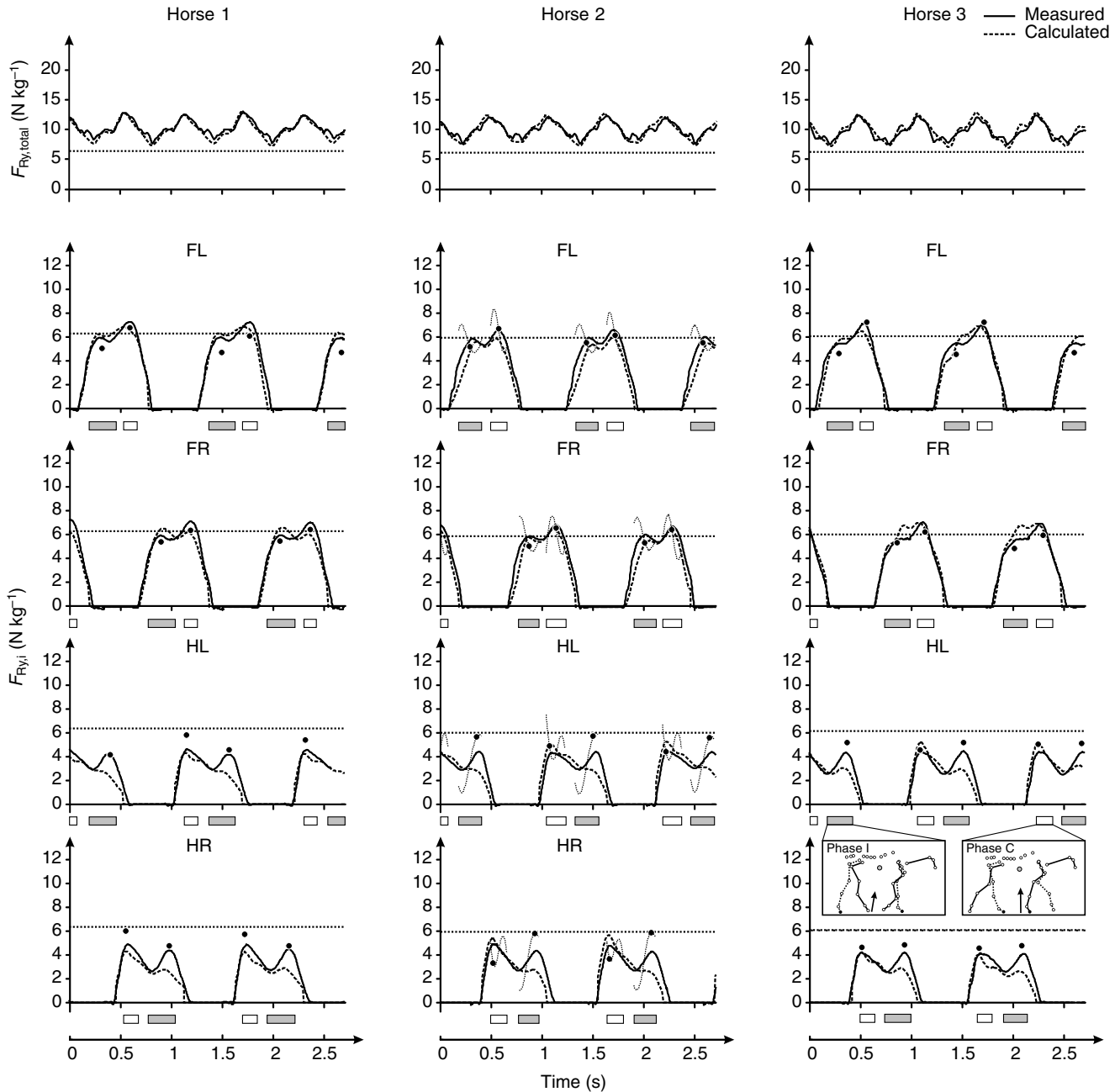


Fig. 3. Time histories of the measured and calculated total vertical ground reaction force ( $F_{Ry,total}$ ), as well as of the measured and calculated vertical ground reaction force on each of the limbs ( $F_{Ry,i}$ ), of three horses at walk. Calculated  $F_{Ry,i}(t)$  were obtained from distal limb lengths, using the force-length relationships of the distal limbs determined with the help of calculated values of  $F_{Ry,i}$  and limb lengths at trot. Dotted horizontal lines indicate half the peak value of  $F_{Ry,total}$ . FL, left forelimb; FR, right forelimb; HL, left hindlimb; HR, right hindlimb. Thin dotted curves in diagrams of horse 2 represent  $F_{Ry,i}$  calculated according to the GRF distribution method for the two phases in each half-cycle in which only two limbs were in contact with the ground (insets in lowermost diagram of horse 3; see legend to Fig. 1 for explanation of information provided in insets), one in which the body is supported by a forelimb and the ipsilateral hindlimb (phase I, grey bars below time axes), and the other in which it is supported by this forelimb and the contralateral hindlimb (phase C, open bars below time axes). Floating dots are values for  $F_{Ry,i}$  extracted from these curves at fixed points during these phases (at 50% of phase I and phase C for the forelimb, at 20% of phase C for the hindlimb and at 80% of phase I for the hindlimb).

needs no argument that the small impact peaks in the measured  $F_{Ry,i}(t)$  of the forelimbs could not be reproduced from the distal limb length-time histories). Fig. 9 shows mean peak measured  $F_{Ry,i}$  values together with mean peak  $F_{Ry,i}$  values calculated

from distal limb length. At trot, the overall correspondence between calculated and measured  $F_{Ry,i}(t)$  was satisfactory, as was to be expected given that peak  $F_{Ry,total}$  could be accurately calculated from kinematics (Fig. 4), that the distribution over

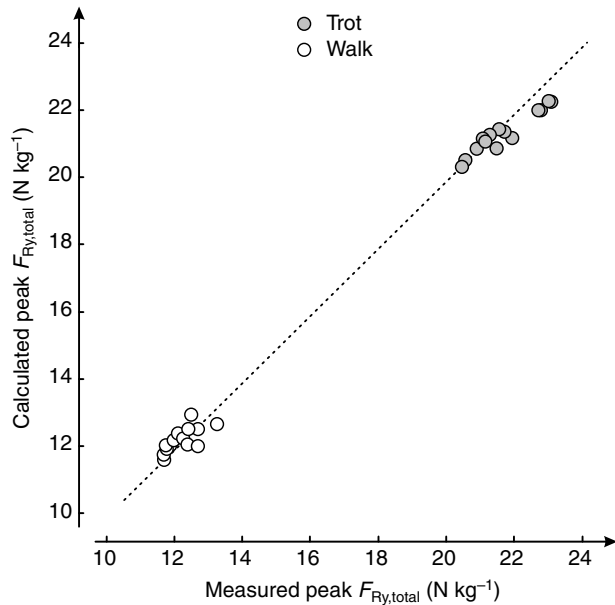


Fig. 4. Mean peak values of the measured and calculated total vertical ground reaction force ( $F_{Ry,total}$ ) at walk and trot. Each point is the average of the peak values of  $F_{Ry,total}$  obtained in several individual stance phases of one horse (15 at trot, nine at walk). Left forelimb stance phases were processed separately from right forelimb stance phases, hence each horse contributed two points at walk and two at trot. The dotted line is the line of identity.

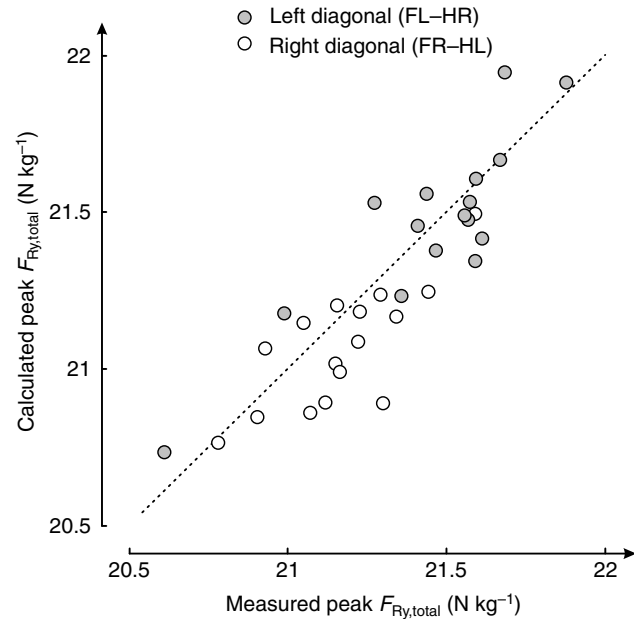


Fig. 5. Peak values of the measured and calculated total vertical ground reaction force ( $F_{Ry,total}$ ) of the individual stance phases of one horse at trot. Left diagonal stance phases (FL–HR) were processed separately from right diagonal stance phases (FR–HL). The dotted line is the line of identity.

the fore- and hindlimbs could be calculated reasonably well (Fig. 6), and that peak  $F_{Ry,i}$  occurred almost at the same time in the forelimb and diagonal hindlimb in contact with the ground (Fig. 2).

At walk, the calculation of  $F_{Ry,total}$  was successful (Figs 3, 4), but the calculation of time histories and peak values of individual limb forces using the GRF distribution method turned out to be quite a challenge. There are two phases in each half-cycle in which the body is supported by only two limbs (insets in Fig. 3 and bars below time axes), one in which the body is supported by a forelimb and the ipsilateral hindlimb (phase I, grey bars in Fig. 3), and the other in which it is supported by this forelimb and the contralateral hindlimb (phase C, open bars in Fig. 3). Unfortunately, in these phases the GRF distribution method produced calculated force–time curves that fluctuated considerably for some of the horses (extreme fluctuations occurring in horse 2 are indicated by thin dotted lines in Fig. 3); obviously, extracting peak values from these curves would produce inaccurate results. What could be done was to extract calculated  $F_{Ry,i}$  values at fixed points in phases I and C (extracting values at 50% of phase I and phase C for the forelimb, at 20% of phase C for the hindlimb and at 80% of phase I for the hindlimb produced the dots in Fig. 3). When we took the largest of these two values for a given limb during its contact phase and averaged them over contact phases, we still did not get a very reliable estimate of the measured mean

peak  $F_{Ry,i}$  of this limb (Fig. 7); the between-limb SEE was  $0.6 \text{ N kg}^{-1}$  for the forelimb but no less than  $1.0 \text{ N kg}^{-1}$  for the hindlimb. Alternatively,  $F_{Ry,i}(t)$  could be calculated from time histories of distal limb length, using the force–length relationships determined on the basis of the results obtained at trot. In the forelimbs,  $F_{Ry,i}(t)$  calculated from distal limb length corresponded quite well with the measured  $F_{Ry,i}(t)$ , but in the hindlimbs the peak in the second half of the stance phase was typically missing (Fig. 3). Nevertheless, both for the forelimbs and for the hindlimbs, the mean peak  $F_{Ry,i}$  calculated from distal limb length corresponded satisfactorily with the mean peak measured  $F_{Ry,i}$  (Fig. 9). The grand mean peak  $F_{Ry,i}$  in the forelimb was calculated to be  $6.9 \pm 0.5 \text{ N kg}^{-1}$  and measured to be  $7.1 \pm 0.3 \text{ N kg}^{-1}$ , with the inter-limb SEE being  $0.4 \text{ N kg}^{-1}$  and the intra-limb SEE amounting to less than  $0.2 \text{ N kg}^{-1}$ . In the hindlimb, the grand mean peak  $F_{Ry,i}$  was calculated to be  $4.8 \pm 0.5 \text{ N kg}^{-1}$  and measured to be  $4.7 \pm 0.3 \text{ N kg}^{-1}$ , with the inter-limb SEE being  $0.5 \text{ N kg}^{-1}$  and the intra-limb SEE amounting to less than  $0.2 \text{ N kg}^{-1}$ . When it comes to estimating the absolute value of peak  $F_{Ry,i}$ , these results compare favourably with the results obtained using the duty factor method; at walk, the grand mean peak  $F_{Ry,i}$ , calculated using Eqn 1 was  $7.6 \pm 0.3 \text{ N kg}^{-1}$  in the forelimb, with the inter-limb SEE being  $0.5 \text{ N kg}^{-1}$ , and  $5.2 \pm 0.3 \text{ N kg}^{-1}$  in the hindlimb, with the inter-limb SEE being  $0.6 \text{ N kg}^{-1}$ . As already pointed out by Witte et al. (Witte et al., 2004), the overestimation of peak  $F_{Ry,i}$  by the duty factor method was due to  $F_{Ry,i}(t)$  departing from the positive half of a sinusoid (Fig. 3).



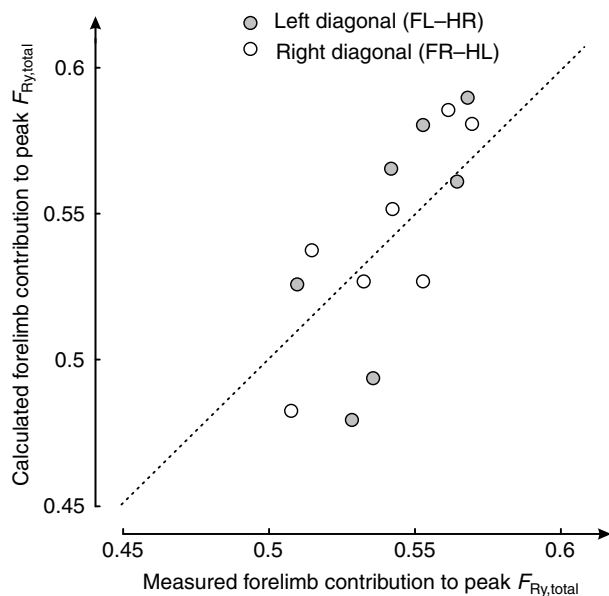


Fig. 6. Mean relative load on the forelimb at the instant that  $F_{Ry,total}$  reached its peak at trot. Left diagonal stance phases (FL–HR) were processed separately from right diagonal stance phases (FR–HL), hence each horse contributed two points. The dotted line is the line of identity.

### Discussion

The purpose of this study was to determine whether the vertical ground reaction forces on the individual limbs ( $F_{Ry,i}$ ) of trotting and walking horses could be accurately calculated from kinematics, without using any information derived from direct force measurements. It was found that  $F_{Ry,i}(t)$  on all limbs could be calculated quite successfully at trot (Fig. 2), and that at walk  $F_{Ry,i}(t)$  could be calculated quite well for the forelimbs but not so well for the hindlimbs (Fig. 3). Nevertheless, at both trot and walk, peak values of  $F_{Ry,i}(t)$  on all limbs (Fig. 9) could be calculated with an inter-limb SEE of  $0.6 \text{ N kg}^{-1}$  or less. Below, we shall first discuss the results of our approach to calculating individual limb forces from kinematics only. Next, we shall address the advantages and disadvantages of the GRF distribution method compared with the duty factor method of calculating individual limb forces, and finally we shall address the potential application of the calculation of individual limb forces from kinematics in studies of locomotor problems.

The GRF distribution method that we proposed is straightforward from a mechanical point of view, and with the precautions taken in this study to reduce errors in the location of bony landmarks due to skin movement, we were able to reliably calculate  $F_{Ry,total}(t)$  both at trot (Fig. 2) and at walk (Fig. 3), and we could calculate peak forces of  $F_{Ry,total}(t)$  with a between-diagonal SEE of  $0.5 \text{ N kg}^{-1}$  or less (Fig. 4). This is of course required for the GRF distribution method to work, but far from sufficient. From Fig. 1, which gives a representative example of the situation at the instant that  $F_{Ry,total}$  reached its peak at trot, it will be obvious that the GRF

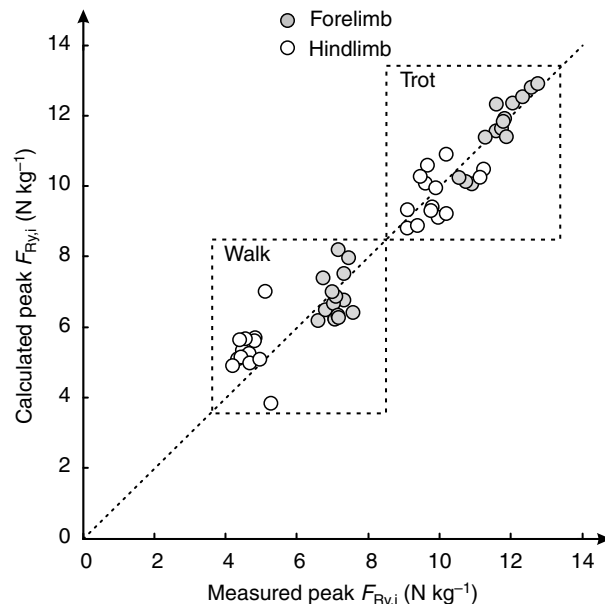


Fig. 7. Mean peak values of the measured and calculated vertical ground reaction forces on the individual limbs ( $F_{Ry,i}$ ) at trot and at walk. Calculated results were obtained using the GRF distribution method; at trot we used the peak value of  $F_{Ry,i}$ , at walk we took the largest one from the two values selected during each stance phase (see Fig. 3). The dotted line is the line of identity.

distribution method also relies critically on the horizontal component of  $F_{R,total}$ , on the exact location of CM, and on the rate of change of angular momentum, which pushes  $F_{R,total}$  away from CM parallel to its line of action. The fact that we were able to accurately calculate the average relative load on the forelimb at the instant that  $F_{Ry,total}$  reached its peak at trot (calculated: 54.1%, measured: 54.3%), suggests that at this instant the horizontal component of  $F_{R,total}$  and the exact location of CM could reliably be obtained from the kinematic data (despite our somewhat bold assumption that the reaction forces on the two limbs in contact were in parallel). The angular momentum was found to be relatively small and unimportant.

Unfortunately, at walk, the GRF distribution method did not work as well as it did at trot. It was not possible to detect a peak in the forces calculated according this method (Fig. 3, diagrams of horse 2), and we had to rely on force values extracted at fixed points in the contact phase of each of the limbs (floating dots in Fig. 3). Although the maximum of these force values did in fact approximate the peak values in the measured forces (Fig. 7), the approach seems quite unreliable if we consider at which point some of the force values were extracted from their corresponding curves (Fig. 3, diagrams of horse 2). Considering that  $F_{Ry,total}$  was approached quite accurately (top panels in Fig. 3), and that also at walk the angular momentum was found to be small and unimportant, it must be concluded that the calculation of the horizontal component of  $F_{R,total}$ , and therewith the point where  $F_{R,total}$  passes between the hoofs, was not very accurate at walk. This

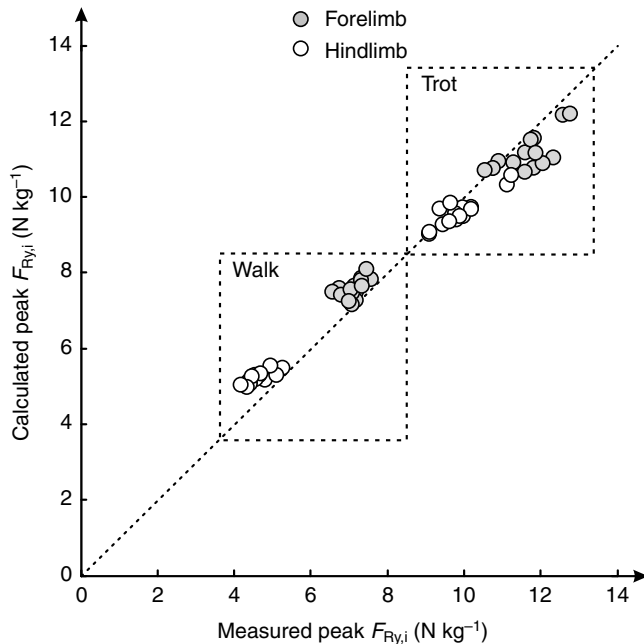


Fig. 8. Mean peak values of the measured and calculated vertical ground reaction forces on the individual limbs ( $F_{Ry,i}$ ) at trot and at walk. Calculated results were obtained using Eqn 1, with duty factors determined from the measured ground reaction forces. The dotted line is the line of identity.

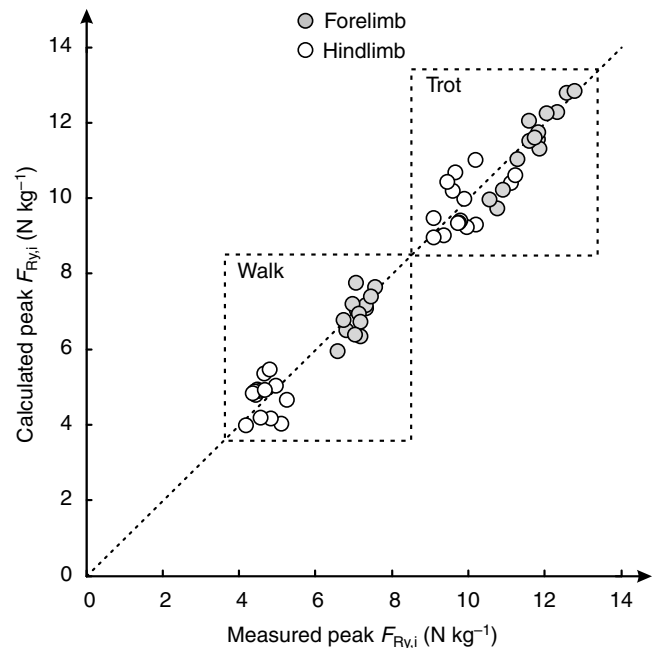


Fig. 9. Mean peak values over the stance phase of the measured and calculated vertical ground reaction forces on the individual limbs ( $F_{Ry,i}$ ) at trot and at walk. Calculated results were obtained from distal limb lengths, using the force-length relationships of the distal limbs determined with the help of calculated values of  $F_{Ry,i}$  and limb lengths at trot. For each horse there are four data points, but some of these are hidden by others. The dotted line is the line of identity.

then brings us to the question how well the individual limb forces calculated from distal limb length compare with measured forces.

The calculation of individual limb forces from distal limb length is based on the notion that the distal limb operates as a linear spring. At trot, a good correspondence was obtained between  $F_{Ry,i}(t)$  calculated from distal limb length and measured  $F_{Ry,i}(t)$  (Fig. 2) and between their mean peak values during the stance phase (Fig. 4), for both the forelimbs and the hindlimbs. However, this is not really surprising. After all, the force-length relationships of the distal limbs were derived using force values and length values calculated at two instants at trot [the instant just before touch-down of the limb and the instant that the calculated  $F_{Ry,total}(t)$  attained its peak]; the crucial information was peak  $F_{R,i}$  calculated according to the GRF distribution method, and we had already established that this method worked well at trot. In any case, the notion that the distal limb operates as a linear spring seems to hold for trotting, for both the forelimbs and the hindlimbs. It is important to note that the stiffness calculated for the 'spring' between elbow and coffin joint varied considerably among the horses participating in this study, from 101 to 156  $\text{N kg}^{-1} \text{m}^{-1}$  (mean, 130  $\text{N kg}^{-1} \text{m}^{-1}$ ), which implies that skipping the calibration step and assuming a fixed value of stiffness for all horses will lead to considerable errors in estimation of  $F_{Ry,i}(t)$ . The stiffness values calculated for the 'spring' between stifle and coffin joint varied less among the horses, from 64 to 78  $\text{N kg}^{-1} \text{m}^{-1}$  (mean, 73  $\text{N kg}^{-1} \text{m}^{-1}$ ).

The problems that we encountered with the GRF distribution method at walk could potentially be solved using the force-length relationships of the distal limbs established on the basis of the results at trot. In the case of the forelimbs,  $F_{Ry,i}(t)$  calculated from distal limb length followed the measured  $F_{Ry,i}(t)$  quite well (Fig. 3). In the case of the hindlimbs, however, the situation was less favourable; the second peak in  $F_{Ry,i}(t)$ , which occurred during the second half of the hindlimb stance phase, was not well reproduced (Fig. 3). It cannot be decided at this point whether this is an artefact due to the specific limb configuration in this phase, causing the fitting of a chain of rigid segments and therewith the determination of limb length to run awry, whether the limb perhaps does not operate like a perfect linear spring with no hysteresis, or whether it is caused by a change in stiffness of the distal hindlimb due to increased muscle activation, which obviously would violate altogether the notion of the distal limb acting as a simple linear spring. Suffice it to say, however, that despite these imperfections the mean peak  $F_{Ry,i}$  during the stance phase calculated from distal limb length corresponded satisfactorily with the mean peak measured  $F_{Ry,i}$ , both for the forelimb and the hindlimb (Fig. 9), with the inter-limb SEE being 0.6  $\text{N kg}^{-1}$  and the intra-limb SEE amounting to less than 0.2  $\text{N kg}^{-1}$ .

Obviously, calculating individual limb forces using the GRF distribution method is highly involved compared to calculating them using the duty factor method. Why go through all the

trouble of collecting and processing the kinematic data, if according to Figs 7 and 8 the duty factor method produces estimates of  $F_{Ry,i}$  that are just as good at trot and perhaps even better at walk? After all, for the duty factor method one only needs touch-down and take-off times of individual hoofs, and these can be determined accurately from hoof-mounted accelerometers (Parsons and Wilson, 2006). If one is interested merely in the ground reaction forces on the individual limbs in healthy animals, the duty factor method is indeed an attractive alternative. Especially at trot, the shape of the individual force curves is virtually identical to the positive half of a sinusoid (Fig. 2) (see also Witte et al., 2004), the motion pattern is left-right symmetrical (the greatest difference that we found in our horses between the mean measured force carried by the left and right side was 2.5% of body weight for the forelimbs and 1.8% of body weight for the hindlimbs), and the assumption of a fixed contribution of the forelimbs and hindlimbs to the average  $F_{Ry,total}$  seems acceptable (the mean contribution of a single forelimb ranged from 0.273 to 0.308 and that from a single hindlimb ranged from 0.20 to 0.227 across the horses used in this study). However, in contrast to the GRF distribution method, the duty factor method crucially relies on information that must have been acquired beforehand with direct force measurements, namely the average contribution of the forelimbs and hindlimbs to the average  $F_{Ry,total}$  at trot and walk. When it comes to studying lame animals, assumptions about left-right symmetry and the contribution of the forelimbs and hindlimbs to the average  $F_{Ry,total}$  will no longer hold (e.g. Weishaupt et al., 2004a; Weishaupt et al., 2006). In that case, the distribution of the average load over the individual limbs is unknown, and its estimation becomes the very challenge. Furthermore, if one wants to study how a horse manages to redistribute the load, information about the forces on the individual limbs is no longer sufficient and kinematic data are needed anyhow. In that case, it is highly desirable to have ground reaction forces on individual limbs that are consistent with the kinematic data, and the GRF distribution method seems to be a suitable way of obtaining these. We are not claiming, of course, that the forces calculated from kinematics could be used for an inverse dynamics analysis; such an analysis requires also the true horizontal component and centre of pressure of the ground reaction forces on each individual limb, which can only be provided by direct measurement with a force plate. At the same time it should not be forgotten, however, that an inverse dynamic analysis can only be conducted reliably if one has a consistent set of kinematic and kinetic data (Bobbert et al., 1991; Bobbert et al., 1992).

The final question is whether the calculation of individual limb forces from kinematics, as proposed in this study, is sufficiently accurate to be used in studying the adaptation of locomotion patterns following injury. Obviously, forces estimated from kinematics will never be as accurate as forces measured directly with a treadmill-integrated system like the one developed by Weishaupt et al. (Weishaupt et al., 2002), but if no direct force measurements are possible the calculation of

individual limb forces from kinematics seems to provide a good alternative. In a study of induced weight-bearing lameness of the forelimb at trot (Weishaupt et al., 2006), it has been shown that horses manage to reduce peak  $F_{Ry,i}$  on the affected limb by 4%, 9% and 24% for subtle, mild and moderate lameness, respectively, with the relative contribution of the forelimb to peak  $F_{Ry,total}$  during the lame diagonal stance phase going down from 53 to 46%. Corresponding values for induced weight-bearing lameness of the hindlimb at trot (Weishaupt et al., 2004a) were 2%, 7% and 15%, respectively, with the relative contribution of the forelimb to peak  $F_{Ry,total}$  during the lame diagonal stance phase going up from 53 to 57%. In these types of studies, changes occur over time and each horse can serve as its own comparison. This means that in calculating the changes in peak  $F_{Ry,i}$  from kinematics as proposed in the current paper, the relevant parameter is the intra-limb SEE, which amounted to less than  $0.2 \text{ N kg}^{-1}$ , i.e. less than 2% of the peak  $F_{Ry,i}$ . It seems, therefore, that the method of calculating peak  $F_{Ry,i}$  from kinematics is sufficiently accurate to study the effects of induced lameness at trot, even if the lameness is only mild to moderate. The method will also be useful for other studies in which each horse can serve as its own comparison, such as studies into the effect of treatment of lameness on the locomotion pattern. The most urgent and perhaps most challenging studies, however, will be those of load distribution in chronically lame horses. For those studies, the method proposed in the present study has the advantage that it does not require the lame horses to walk and trot on an instrumented treadmill, which they might not be able to do, but it remains to be established whether the method is sufficiently accurate to reveal asymmetries in loading of the individual limbs.

In conclusion, the calculation of individual limb reaction forces from kinematics as proposed in the present study is quite accurate: the inter-limb SEE for estimating mean peak forces is of the order of  $0.6 \text{ N kg}^{-1}$ , and the intra-limb SEE is even less than  $0.2 \text{ N kg}^{-1}$ . Apart from that, the approach has an important advantage over other methods, such as the duty factor method: since ground reaction force patterns are calculated from kinematics, one has all the information required for a full biomechanical analysis of the origin of the force patterns, and therefore in the locomotion adaptations responsible for changes in these patterns.

We would like to thank Thomas Wiestner (Vetsuisse Faculty, Zurich) and Christopher Johnston (Swedish University of Agricultural Sciences) for their invaluable help in setting up a project combining kinematic data capture with force measurements by the treadmill-integrated system. We would also like to thank Sören Johansson for providing technical support during the experiments.

## References

- Alexander, R. M., Maloiy, G. M. O., Hunter, B., Jayes, A. S. and Nturi, J. (1979). Mechanical stresses in fast locomotion of buffalo (*Syncerus caffer*) and elephant (*Loxodonta africana*). *J. Zool.* **189**, 135-144.
- Barrey, E. (1990). Investigation of the vertical hoof force distribution in the

- equine forelimb with an instrumented horseboot. *Equine Vet. J. Suppl.* **9**, 35-38.
- Bobbert, M. F. and Santamaria, S.** (2005). Contribution of the forelimbs and hindlimbs of the horse to mechanical energy changes in jumping. *J. Exp. Biol.* **208**, 249-260.
- Bobbert, M. F., Schamhardt, H. C. and Nigg, B. M.** (1991). Calculation of vertical ground reaction force estimates during running from positional data. *J. Biomech.* **24**, 1095-1105.
- Bobbert, M. F., Yeadon, M. R. and Nigg, B. M.** (1992). Mechanical analysis of the landing phase in heel-toe running. *J. Biomech.* **25**, 223-234.
- Buchner, H. H., Savelberg, H. H., Schamhardt, H. C., Merkens, H. W. and Barneveld, A.** (1994). Kinematics of treadmill versus overground locomotion in horses. *Vet. Q.* **16** Suppl. 2, S87-S90.
- Buchner, H. H., Savelberg, H. H., Schamhardt, H. C. and Barneveld, A.** (1996a). Head and trunk movement adaptations in horses with experimentally induced fore- or hindlimb lameness. *Equine Vet. J.* **28**, 71-76.
- Buchner, H. H., Savelberg, H. H., Schamhardt, H. C. and Barneveld, A.** (1996b). Limb movement adaptations in horses with experimentally induced fore- or hindlimb lameness. *Equine Vet. J.* **28**, 63-70.
- Buchner, H. H., Savelberg, H. H., Schamhardt, H. C. and Barneveld, A.** (1997). Inertial properties of Dutch Warmblood horses. *J. Biomech.* **30**, 653-658.
- Buchner, H. H., Obermuller, S. and Scheidl, M.** (2001). Body centre of mass movement in the lame horse. *Equine Vet. J. Suppl.* **33**, 122-127.
- Clayton, H. M., Schamhardt, H. C., Willemen, M. A., Lanovaz, J. L. and Colborne, G. R.** (2000). Kinematics and ground reaction forces in horses with superficial digital flexor tendinitis. *Am. J. Vet. Res.* **61**, 191-196.
- Dutto, D. J., Hoyt, D. F., Cogger, E. A. and Wickler, S. J.** (2004). Ground reaction forces in horses trotting up an incline and on the level over a range of speeds. *J. Exp. Biol.* **207**, 3507-3514.
- Dutto, D. J., Hoyt, D. F., Clayton, H. M., Cogger, E. A. and Wickler, S. J.** (2006). Joint work and power for both the forelimb and hindlimb during trotting in the horse. *J. Exp. Biol.* **209**, 3990-3999.
- Galisteo, A. M., Cano, M. R., Morales, J. L., Miro, F., Vivo, J. and Aguera, E.** (1997). Kinematics in horses at the trot before and after an induced forelimb supporting lameness. *Equine Vet. J. Suppl.* **23**, 97-101.
- Jeffcott, L. B., Rosedale, P. D., Freestone, J., Frank, C. J. and Towers-Clark, P. F.** (1982). An assessment of wastage in thoroughbred racing from conception to 4 years of age. *Equine Vet. J.* **14**, 185-198.
- Kai, M., Aoki, O., Hiraga, A., Oki, H. and Tokuriki, M.** (2000). Use of an instrument sandwiched between the hoof and shoe to measure vertical ground reaction forces and three-dimensional acceleration at the walk, trot, and canter in horses. *Am. J. Vet. Res.* **61**, 979-985.
- Keegan, K. G., Wilson, D. A., Wilson, D. J., Smith, B., Gaughan, E. M., Pleasant, R. S., Lillich, J. D., Kramer, J., Howard, R. D., Bacon-Miller, C. et al.** (1998). Evaluation of mild lameness in horses trotting on a treadmill by clinicians and interns or residents and correlation of their assessments with kinematic gait analysis. *Am. J. Vet. Res.* **59**, 1370-1377.
- Keegan, K. G., Wilson, D. A., Smith, B. K. and Wilson, D. J.** (2000). Changes in kinematic variables observed during pressure-induced forelimb lameness in adult horses trotting on a treadmill. *Am. J. Vet. Res.* **61**, 612-619.
- Kobluk, C. N.** (1998). Epidemiologic studies of racehorse injuries. In *Current Techniques in Equine Surgery and Lameness* (ed. N. A. White and J. M. Moore), pp. 564-569. Philadelphia: W. B. Saunders.
- Kramer, J., Keegan, K. G., Wilson, D. A., Smith, B. K. and Wilson, D. J.** (2000). Kinematics of the hind limb in trotting horses after induced lameness of the distal intertarsal and tarsometatarsal joints and intra-articular administration of anesthetic. *Am. J. Vet. Res.* **61**, 1031-1036.
- McGuigan, M. P. and Wilson, A. M.** (2003). The effect of gait and digital flexor muscle activation on limb compliance in the forelimb of the horse *Equus caballus*. *J. Exp. Biol.* **206**, 1325-1336.
- Merkens, H. W. and Schamhardt, H. C.** (1988). Evaluation of equine locomotion during different degrees of experimentally induced lameness. II: Distribution of ground reaction force patterns of the concurrently loaded limbs. *Equine Vet. J. Suppl.* **6**, 107-112.
- Merkens, H. W., Schamhardt, H. C., Hartman, W. and Kersjes, A. W.** (1986). Ground reaction force patterns of Dutch Warmblood horses at normal walk. *Equine Vet. J.* **18**, 207-214.
- Merkens, H. W., Schamhardt, H. C., van Osch, G. J. and Hartman, W.** (1993a). Ground reaction force patterns of Dutch Warmbloods at the canter. *Am. J. Vet. Res.* **54**, 670-674.
- Merkens, H. W., Schamhardt, H. C., Van Osch, G. J. and Van den Bogert, A. J.** (1993b). Ground reaction force patterns of Dutch warmblood horses at normal trot. *Equine Vet. J.* **25**, 134-137.
- Morris, E. A. and Seeherman, H. J.** (1987). Redistribution of ground reaction forces in experimentally induced equine carpal lameness. In *Equine Exercise Physiology* (ed. J. R. Gillespie and N. E. Robinson), pp. 553-563. Davis, CA: ICEEP Publications.
- Parsons, K. J. and Wilson, A. M.** (2006). The use of MP3 recorders to log data from equine hoof mounted accelerometers. *Equine Vet. J.* **38**, 675-680.
- Roepstorff, L. and Drevemo, S.** (1993). Concept of a force-measuring horseshoe. *Acta Anat. Basel* **146**, 114-119.
- Roland, E. S., Hull, M. L. and Stover, S. M.** (2005). Design and demonstration of a dynamometric horseshoe for measuring ground reaction loads of horses during racing conditions. *J. Biomech.* **38**, 2102-2112.
- Rossdale, P. D., Hopes, R., Wingfield-Digby, N. J. and Offord, K.** (1985). Epidemiological study of wastage among racehorses 1982 and 1983. *Vet. Rec.* **116**, 66-69.
- Schamhardt, H. C. and Merkens, H. W.** (1987). Quantification of equine ground reaction force patterns. *J. Biomech.* **20**, 443-446.
- Schamhardt, H. C., Merkens, H. W. and Lammertink, J. L.** (1986). Software for analysis of equine ground reaction force data. *Comput. Methods Programs Biomed.* **23**, 247-253.
- Uhlir, C., Licka, T., Kubber, P., Peham, C., Scheidl, M. and Girtler, D.** (1997). Compensatory movements of horses with a stance phase lameness. *Equine Vet. J. Suppl.* **23**, 102-105.
- van den Bogert, A. J., Jansen, M. O. and Deuel, N. R.** (1994). Kinematics of the hind limb push-off in elite show jumping horses. *Equine Vet. J. Suppl.* **17**, 80-86.
- van Weeren, P. R. and Barneveld, A.** (1986). A technique to quantify skin displacement in the walking horse. *J. Biomech.* **19**, 879-883.
- van Weeren, P. R., van den Bogert, A. J. and Barneveld, A.** (1988). Quantification of skin displacement near the carpal, tarsal and fetlock joints of the walking horse. *Equine Vet. J.* **20**, 203-208.
- van Weeren, P. R., van den Bogert, A. J. and Barneveld, A.** (1990a). Quantification of skin displacement in the proximal parts of the limbs of the walking horse. *Equine Vet. J. Suppl.* **9**, 110-118.
- van Weeren, P. R., van den Bogert, A. J. and Barneveld, A.** (1990b). A quantitative analysis of skin displacement in the trotting horse. *Equine Vet. J. Suppl.* **9**, 101-109.
- Weishaupt, M. A., Hogg, H. P., Wiestner, T., Denoth, J., Stussi, E. and Auer, J. A.** (2002). Instrumented treadmill for measuring vertical ground reaction forces in horses. *Am. J. Vet. Res.* **63**, 520-527.
- Weishaupt, M. A., Wiestner, T., Hogg, H. P., Jordan, P. and Auer, J. A.** (2004a). Compensatory load redistribution of horses with induced weightbearing hindlimb lameness trotting on a treadmill. *Equine Vet. J.* **36**, 727-733.
- Weishaupt, M. A., Wiestner, T., Hogg, H. P., Jordan, P. and Auer, J. A.** (2004b). Vertical ground reaction force-time histories of sound Warmblood horses trotting on a treadmill. *Vet. J.* **168**, 304-311.
- Weishaupt, M. A., Wiestner, T., Hogg, H. P., Jordan, P. and Auer, J. A.** (2006). Compensatory load redistribution of horses with induced weight-bearing forelimb lameness trotting on a treadmill. *Vet. J.* **171**, 135-146.
- Wilson, A. M., McGuigan, M. P., Su, A. and Van den Bogert, A. J.** (2001). Horses damp the spring in their step. *Nature* **414**, 895-899.
- Witte, T. H., Knill, K. and Wilson, A. M.** (2004). Determination of peak vertical ground reaction force from duty factor in the horse (*Equus caballus*). *J. Exp. Biol.* **207**, 3639-3648.